

# Accurate Frequency Domain Identification of ODEs with Arbitrary Signals

E. Martini, A. V. G. Cavalieri, P. Jordan and L. Lesshafft.

**Abstract**—The control of physical systems, governed by differential equations, frequently requires the identification of dynamical systems. Frequency domain identification has seen much progress over the last decades. Errors due to the usage of arbitrary signals and finite samples, originally understood as leakage errors, were identified as transient effects that can be corrected exactly on discrete systems and asymptotically on sampled continuous system.

We present an alternative exploration of frequency domain identifications errors, by regarding them as spurious inputs which arise as artifacts of signal windowing. A correction procedure for these effects is proposed. Two families of windowing functions are considered, one leading to polynomial, the other to non-polynomial error convergence. The approach resembles the modulating function technique, filtering out the effects of initial conditions, while retaining the spectral interpretation of frequency domain methods and the low computational cost of computing FFTs.

**Index Terms**—IEEE, IEEEtran, journal, L<sup>A</sup>T<sub>E</sub>X, paper, template.

## I. INTRODUCTION

Most physical system are mathematically described by systems of differential equations, whose dynamics can be obtained or modeled by identification techniques: identification of the discretized system, frequency domain identification, modulating functions, among others. Textbook approaches for frequency domain identification involve the application of periodic inputs, allowing for the application of fast and accurate techniques [1]. The use of arbitrary signals requires spurious transients to be accounted for [2].

Here we focus on fully observable, noise-free, systems described by ordinary differential equations. Throughout the work the focus will be kept on linear systems described by

$$\frac{dx}{dt}(t) = Ax(t) + Bu(t), \quad (1)$$

where  $x$  is the state vector,  $u$  the input vector,  $A$  and  $B$  are the system matrices. A generalization for higher-order systems is provided in Section V. The time-continuous system is discretized with  $N$  equally spaced points on a time interval between 0 and  $T$ , with  $t_j = jT/N$ , with corresponding sampling  $f_s = N/T$ , and Nyquist  $f_{nyq} = T/(2N)$  frequencies.

E Martini is with Division of Aeronautical and Aerospace Engineering, Instituto Tecnológico de Aeronáutica, São José dos Campos, SP, Brazil, (e-mail: emartini@ita.br).

A Cavalieri is with the Division of Aeronautical and Aerospace Engineering, Instituto Tecnológico de Aeronáutica, São José dos Campos, SP, Brazil, (e-mail: andre@ita.br).

P Jordan is with the Institute Pprime, Universit de Poitiers, (e-mail: peter.jordan@univ-poitiers.fr).

L Lesshafft is with the Laboratoire d'Hydrodynamique, CNRS / École polytechnique, 91128 Palaiseau, France, (e-mail: lutz@ladhyx.polytechnique.fr).

Time-domain identification consists of estimating matrices  $A$  and  $B$  from  $x(t)$  and  $u(t)$  data, while frequency domain identification approaches the problem via their spectral components  $\hat{x}(f)$  and  $\hat{u}(f)$ . These approaches, although equivalent in theory, have significant practical differences. For instance, colored (non-white noise) inputs generate signals that are correlated in time, and optimal time-domain identification requires the use of full correlation matrices. In the frequency domain each component remains decoupled, which has important practical advantages [3].

A drawback when using frequency domain identification is that finite sampling and data length introduce errors, classically associated with spectral leakage. Reference [2] shows that these errors can be understood as a spurious transient effect, developing an exact correction for discrete and continuous time-domain models. Discrete time-domain formulations can be used to model a discretized version of 1, from which parameters of the continuous systems can be inferred. Alternatively, the continuous time-domain formulation can be used with the sampled data in order to estimate the signals' spectral properties, the latter suffering from errors due to spectral leakage and aliasing. Reference [4] shows that systematic plant estimation errors scale with  $1/N$  when rectangular windows are used, or an improved convergence of  $1/N^2$  when Hanning or *Diff* windows are used.

Focusing on continuous systems, a different approach consists of using modulating functions. The method consists of multiplying 1 by functions with, at least, the first  $n$ -th derivatives are zero, where  $n$  is the differential equation order. Integration by parts eliminates effects of initial conditions and renders a system of linear equations which can be used to estimate elements of  $A$ , while also eliminating the need taking derivatives of system response, which typically increases noise. Various modulating functions were used, such as spline [5], sinusoidal [6], Hermite polynomials [7], wavelets [8] and Poisson moments [9]. Sinusoidal function are typically cheaper, as they allow computation of all modulations with one a fast Fourier transform (FFT). Modulating functions have been used in the identification of integer and fractional order systems [10] and extended to identify both model parameters and model inputs from response observations only [11].

We propose a different interpretation of frequency domain identification errors, relating them to spurious inputs that originate from the windowing process; thus we generalize the results of Pintelon and Shouckens to arbitrary windows. Convergence with respect to sampling frequency is explicitly derived, leading to the proposition of two window families, which show polynomial ( $1/f_s^N \propto 1/N^p$ ) and non-polynomial convergence rates. This approach resembles the

use of modulating functions, is applicable to fractional system and eliminates the effects of initial and boundary conditions.

## II. ERRORS IN FREQUENCY DOMAIN IDENTIFICATION

Frequency domain identification consists in identifying the linear operator of the frequency domain representation of 1,

$$L(f)\hat{x}(f) = B\hat{u}(f), \quad (2)$$

where

$$\hat{x}(f) = \int_{-\infty}^{\infty} x(t)e^{2\pi ift} dt, \quad (3)$$

$$\hat{u}(f) = \int_{-\infty}^{\infty} u(t)e^{2\pi ift} dt, \quad (4)$$

and  $L(f) = 2\pi i - A$ . In practice,  $\hat{x}(f)$  and  $\hat{u}(f)$  are estimated from windowed signals as,

$$\bar{x}(f) = \frac{1}{T} \int_0^T w(t)x(t)e^{2\pi ift} dt \quad (5)$$

$$\bar{u}(f) = \frac{1}{T} \int_0^T w(t)u(t)e^{2\pi ift} dt \quad (6)$$

where  $w(t)$  represents a window function that makes  $(wx)$  and  $(wu)$  integrable. For frequencies  $f = j/NT$ ,  $\bar{x}(f)$  and  $\bar{u}(f)$  coincides with Fourier series coefficients of the periodic extension of  $(wx)$  and  $(wu)$ . These values are typically obtained by performing Fast Fourier Transform on discrete time samples.

Approximation of true Fourier transforms,  $(\hat{\cdot})$ , by transforms of windowed signals,  $(\bar{\cdot})$ , leads to errors due to spectral leakage [12] which can, for instance, mask distinct resonances; implication of such errors for frequency domain system identification were identified and corrected for rectangular windows, by treating them as transient-effects [1, page 206],[2]. Here we derive a generalization of this procedure, in which we replace the transient-effect interpretation by spurious input, allowing for the use of arbitrary windows. Multiplying 1 by the window function  $w(t)$ , gives,

$$w(t)\frac{dx}{dt}(t) = w(t)Ax(t) + w(t)Bu(t), \quad (7)$$

which after manipulation reads,

$$\frac{d(wx)}{dt}(t) = A(t)(wx)(t) + B(t)(wu)(t) + \left(\frac{dw}{dt}x\right)(t). \quad (8)$$

This expression can be viewed as a system equivalent to 1 for a variable  $(wx)(t)$  with an extra input given by  $(\frac{dw}{dt}x)(t)$ . This auxiliary system can be used in order to identify the matrices of the original system in the frequency domain: as  $(wx)(t) \neq 0$  only over a bounded interval, its Fourier Transform can be computed. Integrating 8 for different windows corresponds to the modulating function approach. Instead, here the frequency-domain representation of the equation is obtained via a Fourier transform,

$$L(f)\bar{x}(f) = B\bar{u}(f) + \tilde{x}(f). \quad (9)$$

where,

$$\tilde{x}(f) = \frac{1}{T} \int_0^T \left(\frac{dw}{dt}x\right)(t)e^{2\pi ift} dt. \quad (10)$$

For a rectangular window,

$$\tilde{x}(f) = \frac{1}{T} \int_0^T (\delta(t) - \delta(t-1))x(t)e^{i2\pi ft} dt = \frac{x(0) - x(T)}{T}, \quad (11)$$

where the mismatch between initial and final states (non-periodicity) are responsible for errors, and previously interpreted as transient effects [2]. Note that this term tends to zero as  $T \rightarrow \infty$ . However this convergence is slow, and whenever limited data is available the term might not be negligible. Note also that for  $f = 0$  a equation of the modulating function approach is recovered: the present approach can be regarded as an extension that uses all the spectrum instead of just its first component.

Equation 9 can be used to estimate  $L(f)$ , or equivalently  $A$ ,  $\hat{u}(f)$ , or both at the same time. The latter approach relies on fixing an expansion for  $u(t) = \sum_{i=0}^{n_u} u_i \phi_i(t)$ , and equivalently  $\hat{u}(f) = \sum u_i \hat{\phi}_i(f)$  and a set of  $n_a$  parameters that characterizes  $A$ . Using then  $n_a + n_u$  frequencies as independent equations these parameters can be obtained by solving a linear system of equations, or a least-square estimation if more than  $n_a + n_u$  are considered [11].

Estimation of  $\bar{x}$ ,  $\bar{u}$  and  $\tilde{x}$  from discretized data results in errors due to aliasing effects. To properly access these errors we distinguish between two different types of aliasing: aliasing due to  $\hat{x}$  frequency components above the Nyquist frequency will be refereed as *type I* aliasing. Frequency leakage due to windowing that artificially creates/increases unresolved frequencies will be referred to as *type II* aliasing, which is illustrated in Fig. 1. eqtype I aliasing can be minimized by low-pass filtering both input and output, and will not be further addressed in this study. Type II aliasing also benefits from low-pass filtering  $x(t)$ , but if the window function is not carefully chosen, limited gain is obtained.

Windowing functions are usually designed so as to reduce beam width and side-lobe levels, among other parameters [12]. For our purposes of error correction, windowing functions may be tailored so as to ensure fast convergence of the integrals in 5, 6 and 10. For such cases, analytical expressions for the Fourier transform errors can be derived. The Fourier-series representation of the windowed signal reads,

$$(wx)(t) = \sum_{k=-\infty}^{\infty} a_k e^{2\pi i kt/T}, \quad (12)$$

where the coefficients can be obtained by,

$$a_k = \frac{1}{T} \int_0^T (wx)(t)e^{-2\pi i kt/T} dt, \quad (13)$$

or equivalently by

$$a_k = \int_{-\infty}^{\infty} \hat{w}(f)\hat{x}\left(\frac{kT}{N} - f\right) df. \quad (14)$$

If  $N$ -point discrete Fourier transform coefficients  $a_{k,N}$  are

used to estimate  $a_k$  from  $N$ -point samplings,

$$\begin{aligned} a_{k,N} &= \frac{1}{N} \sum_{j=1}^N (wx) \left( \frac{j}{NT} \right) e^{i2\pi kj/N} \\ &= \sum_{m=-\infty}^{\infty} a_m \frac{1}{N} \sum_{j=1}^N e^{2\pi i(m+k)j/N} \\ &= a_k + \sum_{m=1}^{\infty} (a_{k+mN} + a_{k-mN}), \end{aligned} \quad (15)$$

where the sum in the final line represents the aliasing errors arising from unresolved frequencies (components for which  $|k| > N/2$ ), i.e. the blue region in Fig. 1.

For a band-limited signal, 14 shows that the behavior of the errors,  $a_{k,N} - a_k$ , is given by  $\hat{w}(f)$  for large frequencies: windows for which  $\hat{w}(f)$  decays faster will lead to smaller spectral leakage, and thus to faster convergence of  $a_{k,N}$ . Another insight into the behavior of  $a_k$  can be obtained by consecutive integration by parts of equation 13, which gives, assuming smoothness of  $(wx)(t)$  for  $0 < t < T$ ,

$$a_k = \sum_{j=0}^{\infty} \frac{\frac{d^j(wx)}{dt^j}(T) - \frac{d^j(wx)}{dt^j}(0)}{(2\pi i k)^j}. \quad (16)$$

Thus the leading term for large  $k$  depends on the matching of  $(wx)(t)$ , and its derivatives, at 0 and  $T$ . For large  $m$ ,  $a_{k \pm mN} \approx a_{\pm mN}$ . In 16,  $k$  only appears on the denominator, elevated to  $j$ . As the errors in 15 consist of the sums of the type  $a_k + a_{-k}$ , the sum for odd  $j$ s cancel out. The convergence thus depends on the matching of even derivatives of  $(wx)(t)$ : if  $(wx)(0) = (wx)(T)$ , then  $a_{k+N} + a_{k-N} \propto 1/N^2$ ; if  $\frac{d^2(wx)}{dt^2}(0) = \frac{d^2(wx)}{dt^2}(T)$ , then  $a_{k+N} + a_{k-N} \propto 1/N^4$ , and so forth.

In order to reduce frequency spreading due to the convolution, which leads to type II aliasing, appropriate window functions are tailored in order to smoothly approach 0 at  $t = 0$  and  $t = T$ , thus minimizing derivative mismatch between the beginning and end of the windowed signal.

Note that Fourier-transform errors appear in all terms of 9, but as will be shown later, errors associated with  $\tilde{x}$  typically have slower convergences due to the window derivative being less smooth than the window itself.

### III. PROPOSED WINDOWS

As long as  $T$ -periodic inputs are fed into 1, matching of  $(wx)(t)$  and all its derivatives at  $t = 0$  and  $t = T$  is guaranteed, with fast convergence due to 16. Dealing with arbitrary signals, the only way to ensure these matchings is to choose a window such that  $w(0) = w(T) = 0$ , which guarantees that windowed signals have null values at the start and end of the window. Similarly, as

$$\frac{d^p wx}{dt^p}(t) = \sum_{i=0}^p \binom{i}{p} \frac{d^i w}{dt^i}(t) \frac{d^{i-p} x}{dt^{i-p}}(t), \quad (17)$$

the  $n$ -th derivative of  $(wx)(t)$  at 0 and  $T$  are only guaranteed to match if  $\frac{d^j w}{dt^j}(0) = \frac{d^j w}{dt^j}(T) = 0$  for all  $j \leq n$ . We thus propose the use of two window families for system identification,

$$w_{\sin^n}(t) = \sin^n(\pi t/T), \quad (18)$$

whose first  $n - 1$  derivatives are zero at 0 and  $T$ , and

$$w_{C_n^\infty}(t) = e^{\frac{nT}{t(T-t)}} / e^{4n}, \quad (19)$$

whose derivatives are all zero at 0 and  $T$ .

These windows, illustrated in Fig. 2, render, respectively, polynomial and non-polynomial convergence rates. The  $w_{\sin^n}$  window family is not new:  $w_{\sin^1}$  corresponding to sine (sometimes referred to as cosine) window;  $w_{\sin^2}$  to the Hann window; and  $w_{\sin^n}$  as the  $\cos^\alpha$  window [12]. The fast spectral decay for large frequencies was already explored in this reference four decades ago: it is remarked in that spectral leakage is minimized by setting window values and their derivatives to zero at the window extremes, but to the best of authors' knowledge this approach has never been applied to identification via frequency domain or modulating function: recent frequency domain studies employ rectangular windows [13], and modulating functions are usually taken to have derivatives vanishing only up to the equations order [11]. The authors are also unaware of the use of windows whose derivatives are all equal to zero, as in  $w_{C_n^\infty}$ .

Error estimation can be derived from a band-limited signal with  $\hat{x}(|f| > f_{max}) = 0$ . Neglecting cancellations between  $a_{k \pm N}$  terms, the error,  $a_{k,N} - a_k$ , is on the order of  $\max(|a_{k+N}|, |a_{k-N}|)$ , where

$$a_{k \pm N} = \int_{-f_{max}}^{f_{max}} \hat{w}(k \pm N - f) \hat{y}(f) df \quad (20)$$

We define  $f_p^{err}$  as being the the smallest frequency for which  $|w(|f| > f_p^{err})|/S < p$ , where  $S$  is the area under the window, following [12]. Thus, by choosing  $N$  such that  $|k \pm (N - f_{max})| > f_p^{err}$ , the influence of each frequency component of  $\hat{x}(f)$  on  $a_{k \pm N}$  is smaller than  $p$ . The process is illustrated in Fig. 3, and  $f_p^{err}$  values are provided in table I.

Note that  $f_p^{err}$  provides only an error estimate, the true error being given by the sum in the last line of 15. In particular, for even order  $w_{\sin^n}$ , cancellation between  $a_{k+N}$  and  $a_{k-N}$  becomes significant for large  $N$ , as indicated by Fig. 4.

### IV. EXAMPLES ON TEST PLANTS

We illustrate here the window implementation with a system described by 1, with  $x(t)$  and  $u(t)$  being vectors of size 9, and  $A$  and  $B$  are matrices with random entries, normally distributed with zero mean and unitary standard variation. A harmonic, non-periodic forcing on the interval  $t \in (0, 1)$ , is used; with  $u(t) = \exp(i\sqrt{2}t)$ . The initial condition  $x(0)$  are taken as a random distributed vector with a standard variation of  $10^3$ : this choice is made such as to focus on the window performance on filtering out initial conditions from the forced signal.

The estimation errors associated with the use of  $w_{\sin^n}$  and  $w_{C_n^\infty}$  are seen in figures 5 and 6, confirming the theoretical

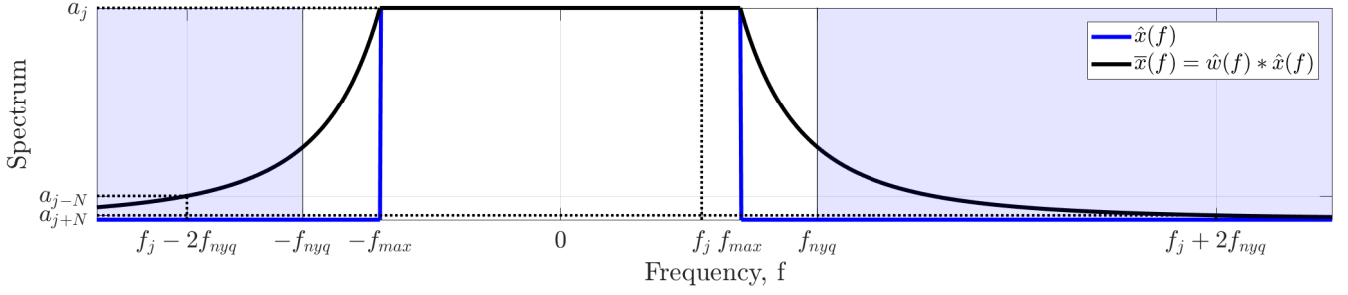


Fig. 1. Aliasing error of windowed signals. A window function  $w$  is applied to a band limited signal (blue line representing its frequency content), resulting in spectral leakage, which spreads the frequency content of the signal (shown in black). The signal is sampled with Nyquist frequency  $f_{nyq} = N/2T$ ; blue region indicate unresolved frequencies. The frequency content at  $f_j = j/T$ ,  $a_j$ , and its aliased components  $a_{j+N}$ ,  $a_{j-N}$  are indicated.

TABLE I  
VALUES OF  $f_p^{err}$  FOR THE PROPOSED WINDOWS .

	Window			Window Derivative			Window 2nd Derivative			Window 3rd Derivative		
	$f_{10^{-3}}^{err}$	$f_{10^{-6}}^{err}$	$f_{10^{-12}}^{err}$	$f_{10^{-3}}^{err}$	$f_{10^{-6}}^{err}$	$f_{10^{-12}}^{err}$	$f_{10^{-3}}^{err}$	$f_{10^{-6}}^{err}$	$f_{10^{-12}}^{err}$	$f_{10^{-3}}^{err}$	$f_{10^{-6}}^{err}$	$f_{10^{-12}}^{err}$
$w_{\sin^1}$	16	502	>10000	1637	>10000	>10000	50	1626	>10000	5191	>10000	>10000
$w_{\sin^2}$	7	68	4911	45	1453	>10000	>10000	>10000	>10000	281	5191	>10000
$w_{\sin^3}$	5	28	867	16	153	>10000	150	>10000	>10000	>10000	>10000	>10000
$w_{\sin^4}$	4	17	264	10	53	1683	37	369	>10000	564	>10000	>10000
$w_{\sin^5}$	5	13	124	8	30	467	20	109	3491	96	956	>10000
$w_{\sin^7}$	5	10	51	7	17	116	12	35	346	26	102	1607
$w_{C_{0.25}^\infty}$	12	45	191	34	99	320	93	198	507	202	354	760
$w_{C_1^\infty}$	7	19	64	14	33	95	28	55	136	50	88	187
$w_{C_2^\infty}$	7	15	41	11	22	57	19	34	77	30	50	103
$w_{C_3^\infty}$	7	13	33	10	19	44	16	27	58	24	38	76
$w_{C_4^\infty}$	7	13	30	10	18	39	15	24	50	21	33	63

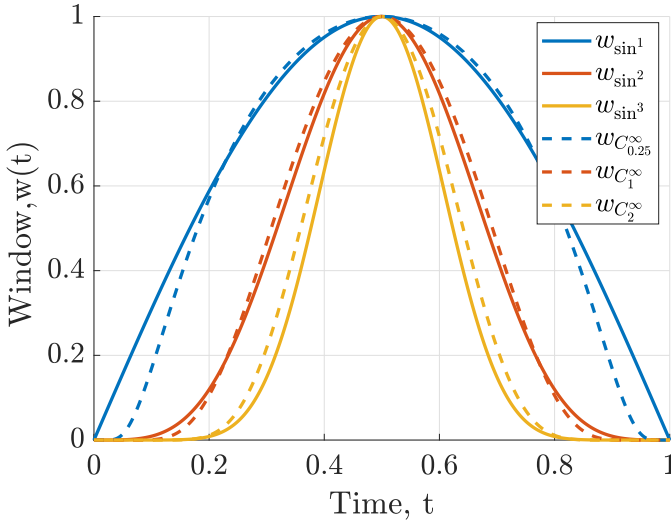


Fig. 2. Proposed windows:  $w_{\sin^n}(t)$  and  $w_{C_n^\infty}(t)$ .

polynomial and exponential, convergence rates. Clearly low order windows need much larger frequency sampling rates in order to filter out initial conditions; the proposed higher-order windows have faster convergence of error and allow accurate system identification with significantly lower sampling requirements. A similar effect is found whenever  $|x| \gg |u|$ , which can occur due to large initial conditions, as before mentioned; due to large gains, where gains are defined as  $|x|/|u|$ ; or due to the presence of resonances or instabilities:

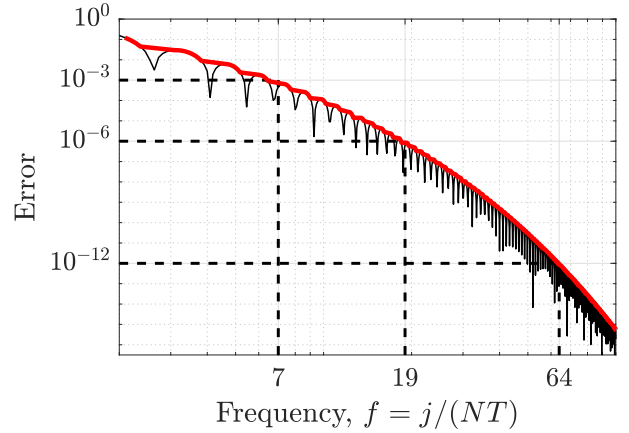


Fig. 3. Illustration of the determination of  $f_p^{err}$  for the  $w_{C_1^\infty}$  window. Black lines correspond to  $\hat{w}(f)/S$ , where  $S$  is the window area. Red line indicates the error envelope and dashed error levels and their corresponding  $f_p^{err}$ .

as the correction term is proportional to  $x$ , the correction term  $\tilde{x}$  needs to be accurately calculated in order for  $B\tilde{u}$  to be accurately determined.

The window spectral properties, such as beam-width dynamic-range, needs to be addressed in order to avoid masking of distinct, but close, peaks; or creation of spurious secondary peaks, as discussed in [12]. Higher-order windows will lead to lower-frequency resolution, which is associated with a poorer usage of window data: higher-order windows have near-zero values on a significant portion of the interval, which is a

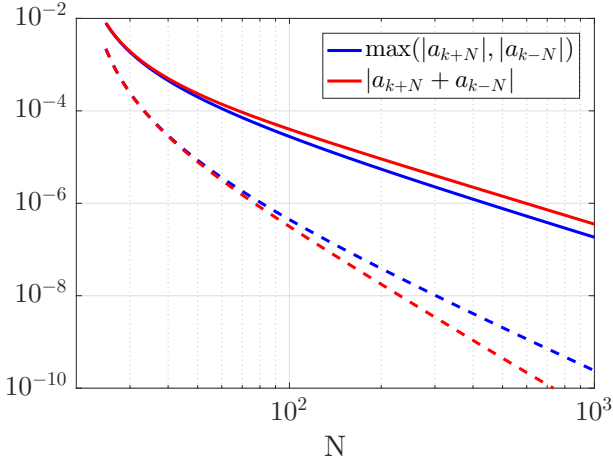


Fig. 4. Illustration of the different behavior of  $|a_{k \pm N}|$  and of  $|a_{k+N} + a_{k-N}|$  for large  $N$ . For  $w_{\sin^1}$ ,  $|a_{k+N} + a_{k-N}| \approx 2|a_{k \pm N}|$  (solid lines); while the  $w_{\sin^2}$ ,  $|a_{k+N} + a_{k-N}| \ll 2|a_{k \pm N}|$  (dashed lines).

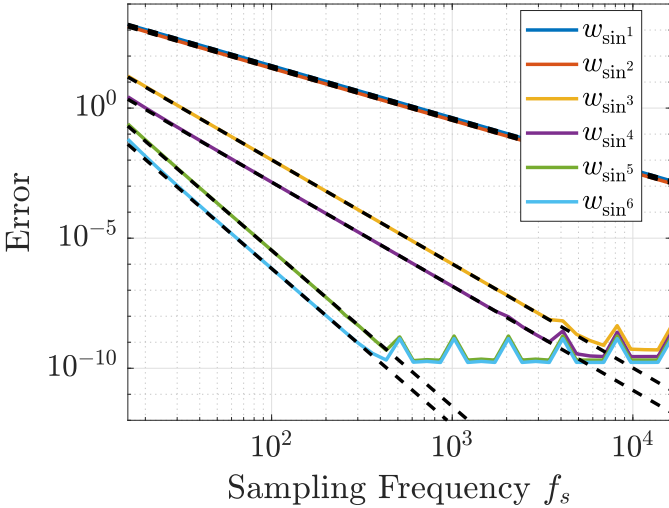


Fig. 5. Aliasing error,  $|B\bar{u} - (L\bar{x} - \bar{x})|/|B\bar{u}|$ , showing a polynomial convergence rate for the  $w_{\sin^n}$  window family, each pair of dashed lines corresponds to  $1/f_s^2$ ,  $1/f_s^4$ , and  $1/f_s^6$ , respectively. Results for  $f = 3$  ( $a_3$ ), for a system driven by a harmonic input with  $\exp(i\sqrt{2}t)$  time dependence.

clear trade-off with their improved convergence rate. In a periodogram approach, the penalty of this trade-off can be alleviated by window overlap. The typical motivation for window overlap is to increase the number of samples for averaging, or alternatively, increase the samples length, as illustrated on Fig. 7. This approach comes with the drawback of creating artificial correlation between samples. Assuming a Gaussian process and a flat spectral content, the power spectrum standard variation can be estimated as [14]

$$\frac{\text{Var}\{\hat{x}^2\}}{\text{E}^2\{\hat{x}\}} = \frac{\left(1 + 2 \sum_{j=1}^{K-1} \frac{K-j}{K} \rho_j\right)}{K} \approx \frac{\left(1 + 2 \sum_{j=1}^{K-1} \rho_j\right)}{K} \quad (21)$$

where

$$\rho_j = \left( \frac{\int w(t)w(t-jT(1-\text{overlap}))dt}{\int w^2(t)dt} \right)^2, \quad (22)$$

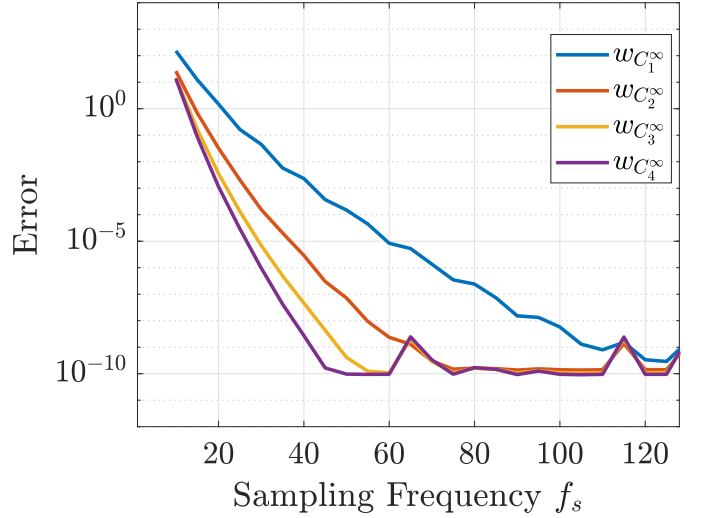


Fig. 6. Same as Fig. 5 for the  $w_{C_n^\infty}$  window family.

$K \approx \frac{L}{T(1-\text{overlap})}$  is the total number of samples,  $L$  length of available data and  $T$  the window length. The approximation corresponds to the limit where  $K \gg 1/\text{overlap}$ , implying  $\rho_j = 0$  for  $j \gg 1$ .

Detailed relations between correlation and window overlap, for a broad class of windows, is available in the literature [12]. Fig. 8 shows the reduction in standard variation, for a given  $L$ , when overlap is used for the windows here studies and for  $W_n(t) = 1 - (t - 0.5)^n$  for  $0 < t < 1$ , for reference. Higher order windows require larger overlaps in order for the variance to converge to its minimum value, which is related to their lesser use of window data. Multiplying the variance by windows half-power width, a measure of the variance in terms of a effective window size is obtained. In terms of these metric, all windows approximately converge to the same variance. For windows the proposed windows with  $n \leq 4$ , a 80% overlap guarantees good convergence on the estimation variance.

The method here proposed has low computational cost, as only time domain multiplication and Fourier transforms, are necessary. All derivatives are either transferred to the window function, which is known analytically, or computed exactly in the frequency domain.

## V. GENERALIZATION TO HIGHER-ORDER DIFFERENTIAL-EQUATION IDENTIFICATION

An  $n$ -th order input-output system is defined as

$$\sum_{j=0}^{n_x} A_j \frac{d^j x}{dt^j} = \sum_{j=0}^{n_u} B_j \frac{d^j u}{dt^j}. \quad (23)$$

In the same way as demonstrated for the first-order system in Sec II, its windowed frequency-domain representation is

$$\sum_{j=0}^{n_x} (i\omega)^j A_j \bar{x} - \sum_{j=0}^{n_u} (i\omega)^j B_j \bar{x} = \sum_{j=0}^{n_x} A_j \hat{x}^{(j)} - \sum_{j=0}^{n_u} B_j \hat{u}^{(j)}, \quad (24)$$

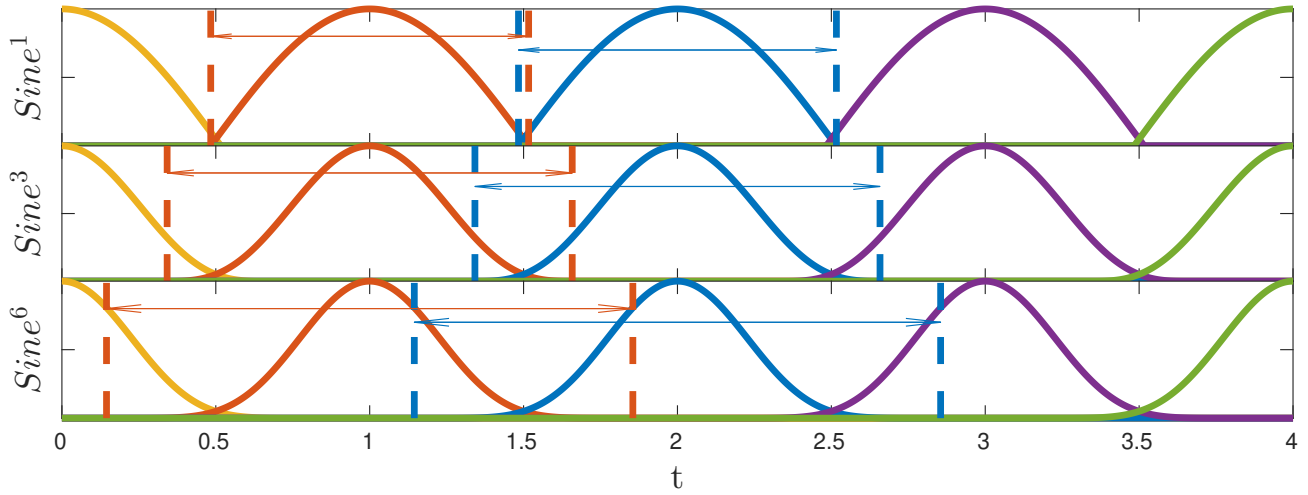


Fig. 7. Comparison of different order  $w_{\sin^n}$  windows. Note high order windows can have significant overlaps (window size indicated by the arrows), without their signals having significant correlations.

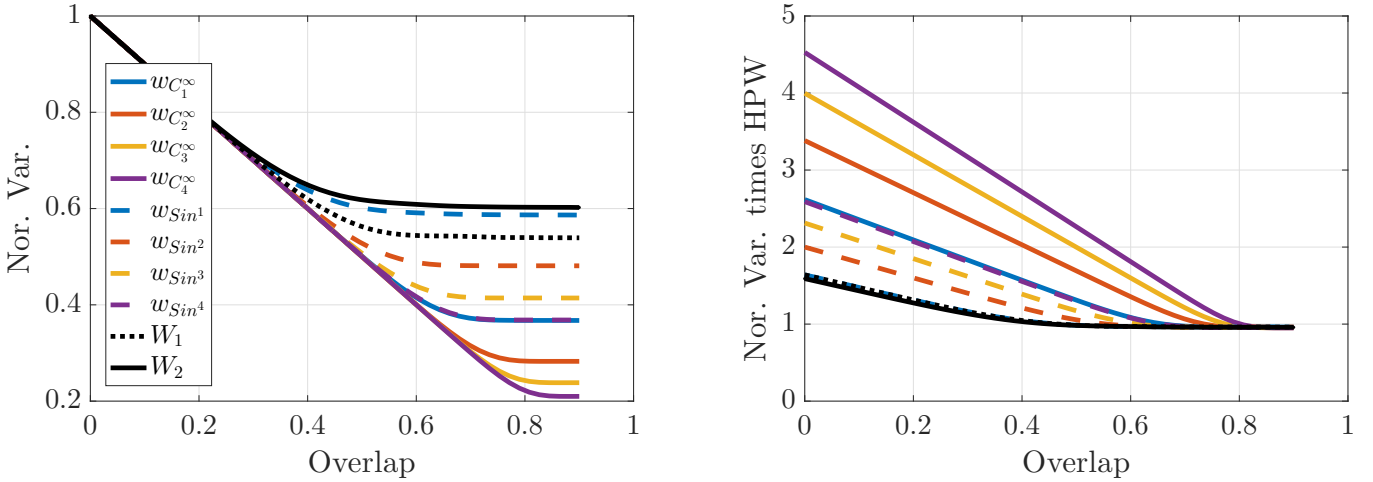


Fig. 8. Variance reduction due to overlap. On the left variance is normalized by the zero overlap value (Nor. Var.), on the left this normalized value is multiplied by each window half-power width (HPW).

where  $\bar{x}$  is defined as in 5, and

$$\tilde{x}^{(j)} = \int_0^T x^{(j)}(t) dt, \quad (25)$$

$$x^{(j)} = \frac{d^j(wx)}{dt^j} - w \left( \frac{d^j x}{dt^j} \right), \quad (26)$$

with equivalent expressions for  $u^{(j)}$ .

Note that  $\tilde{x}^{(1)} = \tilde{x}$ , as defined by 10. It is necessary to express  $x^{(i)}$  as a sum of terms of the form,  $\frac{d^m}{dt^m} \left( \frac{d^k w}{dt^k} x \right)$ , such that no derivatives of  $x$  are necessary: all derivatives should be found on the window, and are obtained analytically, or apply on the product of the window and signal, corresponding to a multiplication on the frequency domain. The errors associated with numerically computing derivatives from sampled data are therefore avoided. A recurrence relation for  $x^{(j)}$  is derived,

with results for  $u^{(j)}$  being analogous. By noting that,

$$\begin{aligned} \frac{d^j x^{(i)}}{dt^j} &= \frac{d^{i+j}(wx)}{dt^{i+j}} - \frac{d^j(w d^i x / dt^i)}{dt^j} \\ &= \sum_{k=1}^{i+j} \left( \binom{k}{i+j} - \binom{k}{j} \right) \frac{d^k w}{dt^k} \frac{d^{i+j-k} x}{dt^{i+j-k}}, \end{aligned} \quad (27)$$

where  $\binom{i}{j}$  is the binomial of  $i$  and  $j$ , with the convention that  $\binom{i}{j} = 0$  for  $i < 0$  or  $i > j$ , and that it is possible to solve,

$$\sum_{j=0}^{n-1} a_j \frac{d^j x^{(n-j)}}{dx^j} = \frac{d^n w^n}{dx^n} x, \quad (28)$$

a linear system

$$\sum_{j=0}^{n-1} A_{i,j} a_j = \delta_{i,n}, \quad (29)$$

$$A_{i,j} = \binom{i}{n} - \binom{i}{j}. \quad (30)$$

Solving for  $a_j$  allows  $x^{\{i\}}$  to be obtained as

$$x^{\{i\}} = \frac{1}{a_0} \left( \frac{d^i w}{dt^i} x + \sum_{j=1}^{i-1} a_j \frac{d^j x^{\{i-j\}}}{dt^j} \right). \quad (31)$$

The first three correction terms can be computed as

$$x^{\{1\}} = \frac{dw}{dt} x, \quad (32)$$

$$x^{\{2\}} = -\frac{d^2 w}{dt^2} x + 2 \frac{dx^{\{1\}}}{dt}, \quad (33)$$

$$x^{\{3\}} = \frac{d^3 w}{dt^3} x + 3 \frac{dx^{\{2\}}}{dt} - 3 \frac{d^2 x^{\{1\}}}{dt^2}, \quad (34)$$

with corresponding frequency counterparts,

$$\tilde{x}^{\{1\}} = F \left( \frac{dw}{dt} x \right), \quad (35)$$

$$\tilde{x}^{\{2\}} = -F \left( \frac{d^2 w}{dt^2} x \right) + 2(2\pi i) \tilde{x}^{\{1\}}, \quad (36)$$

$$\tilde{x}^{\{3\}} = F \left( \frac{d^3 w}{dt^3} x \right) + 3(2\pi i) \tilde{x}^{\{2\}} - 3(2\pi i)^2 \tilde{x}^{\{1\}}, \quad (37)$$

where  $F$  represents Fourier transforms.

Expressions for the first three window derivatives for  $T = 1$  are given in 38-45, and illustrated in Fig. 9.

## VI. CONCLUSION

A new interpretation of windowing errors in frequency domain-identification has been proposed, together with a correction technique applicable to arbitrary windows functions. The method has properties from frequency domain identification, such as the low computational cost of FFTs, and from the modulating function method, such as the filtering of initial conditions. Two types of windows were explored, one yielding polynomial and the other non-polynomial error convergence with sampling frequency. In noise-free systems this leads to high identification accuracy, with particular relevance for the analysis of numerical simulation data, where noise levels are small or nonexistent, and for high-gain systems, where, as  $x$  larger is than  $u$ , errors in  $\tilde{x}$  may dominate the signal. Multi-dimensional systems can be identified by using external products of the proposed windows, such as  $w_{2D}(x, y) = w_{C_n^\infty}(x)w_{C_n^\infty}(y)$ , as in [15].

The approach also allows for improved accuracy in systems with noise. Random noise with zero mean is typically dealt with by sample averaging, as it will average out with a sufficiently large number of samples. However, as windowing errors do not have zero mean, a trade off between windowing error and noise needs to be achieved. Reducing windowing error allows for the use of smaller windows, increasing the number of uncorrelated samples available for averaging.

Finally, for higher-order systems, the  $w_{C_n^\infty}$  window family presented here allows for accurate identification, requiring low oversampling for aliasing error convergence even on higher order systems.

## ACKNOWLEDGMENT

E. Martini acknowledges financial support from CAPES (grant number 88881.190271/2018-01), and would like to thank Daniel Rodrigues, from Universidade Federal Fluminense, for discussion and suggestion provided.

## REFERENCES

- [1] R. Pintelon and J. Schoukens, *System identification: a frequency domain approach*. John Wiley & Sons, 2012.
- [2] R. Pintelon, J. Schoukens, and G. Vandersteen, "Frequency domain system identification using arbitrary signals," *IEEE Transactions on Automatic Control*, vol. 42, no. 12, pp. 1717–1720, 1997.
- [3] T. McKelvey, "Frequency domain identification," in *Preprints of the 12th IFAC symposium on system identification, Santa Barbara, USA*, 2000.
- [4] J. Schoukens, Y. Rolain, and R. Pintelon, "Leakage reduction in frequency-response function measurements," *IEEE transactions on instrumentation and measurement*, vol. 55, no. 6, pp. 2286–2291, 2006.
- [5] H. Preisig and D. Rippin, "Theory and application of the modulating function method. review and theory of the method and theory of the spline-type modulating functions," *Computers & chemical engineering*, vol. 17, no. 1, pp. 1–16, 1993.
- [6] B. Ydstie *et al.*, "System identification using modulating functions and fast fourier transforms," *Computers & chemical engineering*, vol. 14, no. 10, pp. 1051–1066, 1990.
- [7] K. Takaya, "The use of hermite functions for system identification," *IEEE Transactions on Automatic Control*, vol. 13, no. 4, pp. 446–447, 1968.
- [8] M. S. Sadabadi, M. Shafiee, and M. Karrari, "System identification of two-dimensional continuous-time systems using wavelets as modulating functions," *ISA transactions*, vol. 47, no. 3, pp. 256–266, 2008.
- [9] D. C. SAHA, B. P. RAO, and G. P. RAO, "Structure and parameter identification in linear continuous lumped systems the poisson moment functional approach," *International Journal of Control*, vol. 36, no. 3, pp. 477–491, 1982.
- [10] P. Nazarian, M. Haeri, and M. S. Tavazoei, "Identifiability of fractional order systems using input output frequency contents," *ISA transactions*, vol. 49, no. 2, pp. 207–214, 2010.
- [11] S. Asiri and T.-M. Laleg-Kirati, "Modulating functions-based method for parameters and source estimation in one-dimensional partial differential equations," *Inverse Problems in Science and Engineering*, vol. 25, no. 8, pp. 1191–1215, 2017.
- [12] F. J. Harris, "On the use of windows for harmonic analysis with the discrete fourier transform," *Proceedings of the IEEE*, vol. 66, no. 1, pp. 51–83, 1978.
- [13] J. Goos, J. Lataire, E. Louarroudi, and R. Pintelon, "Frequency domain weighted nonlinear least squares estimation of parameter-varying differential equations," *Automatica*, vol. 75, pp. 191 – 199, 2017. [Online]. Available: <http://www.sciencedirect.com/science/article/pii/S0005109816303764>
- [14] P. Welch, "The use of fast fourier transform for the estimation of power spectra: a method based on time averaging over short, modified periodograms," *IEEE Transactions on audio and electroacoustics*, vol. 15, no. 2, pp. 70–73, 1967.
- [15] S. Asiri and T.-M. Laleg-Kirati, "Source estimation for the damped wave equation using modulating functions method: Application to the estimation of the cerebral blood flow," *IFAC-PapersOnLine*, vol. 50, no. 1, pp. 7082 – 7088, 2017, 20th IFAC World Congress. [Online]. Available: <http://www.sciencedirect.com/science/article/pii/S2405896317318918>

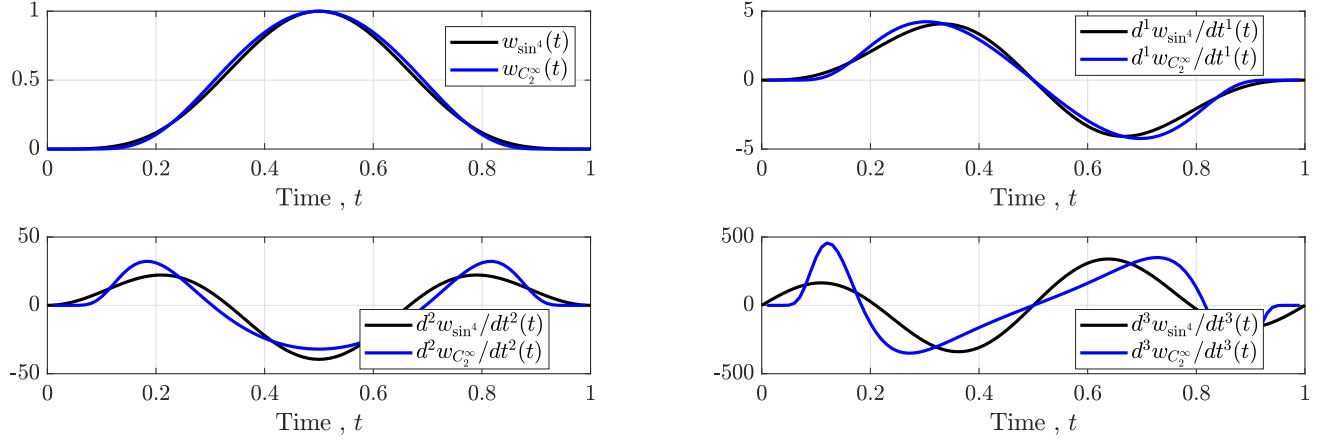


Fig. 9. Illustration windows and their time derivatives.

$$w_{C_n^\infty}(t) = \frac{e^{\frac{n}{t(1-t)}}}{e^{4n}} \quad (38)$$

$$\frac{dw_{C_n^\infty}}{dt}(t) = -\frac{(2nt - n)}{t^2(t-1)^2} \frac{e^{\frac{n}{t(1-t)}}}{e^{4n}} \quad (39)$$

$$\frac{d^2 w_{C_n^\infty}}{dt^2}(t) = \frac{(6nt^4 - 12nt^3 + (4n^2 + 8n)t^2 + (-4n^2 - 2n)t + n^2)}{t^4(t-1)^4} \frac{e^{\frac{n}{t(1-t)}}}{e^{4n}} \quad (40)$$

$$\frac{d^3 w_{C_n^\infty}}{dt^3}(t) = \frac{n(2t-1)(12t^6 - 36t^5 + 18nt^4 + 42t^4 - 36nt^3 - 24t^3 + 4n^2t^2 + 24nt^2 + 6t^2 - 4n^2t - 6nt + n^2)}{(t-1)^6 t^6} \frac{e^{\frac{n}{t(1-t)}}}{e^{4n}} \quad (41)$$

$$w_{\sin^n}(t) = \sin^n(\pi t) \quad (42)$$

$$\frac{dw_{\sin^n}}{dt}(t) = n\pi \cos(\pi t) \sin^{n-1}(\pi t) \quad (43)$$

$$\frac{d^2 w_{\sin^n}}{dt^2}(t) = -n\pi^2 \sin^{n-2}(\pi t)(n \sin^2(\pi t) + (1-n)) \quad (44)$$

$$\frac{d^3 w_{\sin^n}}{dt^3}(t) = -n\pi^3 \sin^{n-3}(\pi t)(n^2 \cos(\pi t) \sin^2(\pi t) + (-n^2 + 3n - 2) \cos(\pi t)) \quad (45)$$



**E. Martini** was born in So Paulo, SP, Brazil in 1984. He is currently a Ph.D. laureate at the Instituto Tecnológico de Aeronáutica. He has a B.A. (2007) from the Federal University of So Carlos, and a Msc (2010) from Chalmers University of Technology, and worked as a Development Engineer at Embraer for 6 years. His currently research interests are in fluid mechanics, focusing on fundamentals of instability mechanisms, control and signal processing tools.



**Andr V. G. Cavalieri** was born in Vila Velha, Brazil, in 1982. He is currently an associate professor at Instituto Tecnológico de Aeronáutica (ITA). He has B.S. (2004) and MSc. (2006) degrees from ITA, and a PhD (2012) from Université de Poitiers, followed by a post-doc in the University of Cambridge. His main research interests are in fluid mechanics, focusing on flow instability, turbulence and aeroacoustics, and also on the development of signal processing to extract the relevant features of complex flows.





**Peter Jordan** was born in Cork, Ireland, in 1974. He received his B.A. and B.A.I. degrees, in Mathematics and Mechanical Engineering, respectively, from Trinity College Dublin, Ireland, in 1996 and his Ph.D, also from TCD, in 2001. He has been a CNRS researcher at the PPRIME Institute (formerly Laboratoire d'Etudes Aérodynamiques), Poitiers, France since 2001.



**Lutz Lesshaft** , born in Berlin, Germany, in 1975, is a CNRS researcher at the Laboratoire d'Hydrodynamique in Palaiseau, France, and a teaching professor at École polytechnique. He holds Master degrees in Mechanical Engineering from the University of Michigan (2001) and from TU Berlin (2002). He received his Ph.D. from École polytechnique in 2006, and was a postdoc at UC Santa Barbara.